# Beam Based Alignment of the TESLA X-ray FEL undulators

B. Faatz

*Deutsches Elektronen-Synchrotron (DESY), Notkestr. 85, 22607 Hamburg, Germany*

**Abstract**

One of the important parameters that determine the performance of the FEL is the overlap between electron beam and radiation field during the amplification process. An earlier study has shown that in order to maintain this overlap, quadrupoles have to be aligned with an accuracy of 1 $\mu$m. In addition, first and second field integrals of the magnetic structures have to be corrected. Since this cannot be done by conventional alignment techniques, beam based alignment will be used to determine steerer settings to correct offsets of quadrupoles and first and second magnetic field integrals.

In this report, all the steps needed to align the electron beam are discussed. Results of simulations of the final alignment are shown. Parameters that limit the alignment will be addressed.

## 1. Introduction

The TESLA X-ray FEL laboratory is a proposed user facility in the wavelength range between $0.85$ Å and 6 nm. The longest wavelength is about equal to the shortest wavelength produced by the TESLA Test Facility (TTF) FEL, under construction at DESY [1]. Similar to the TTF-FEL, the TESLA X-ray FEL is an FEL that employs the principle of Self Amplified Spontaneous Emission (SASE), in which the radiation is built up from the shotnoise produced by the electron beam in a single pass through the undulator. This scheme is used because no high reflectivity mirrors are available in this wavelength range.

The layout of the X-ray FEL is shown in Fig. 1. The electron beam produced by the accelerator will have an energy between 15 and 50 GeV, distributed over two beam lines, one in the energy range from 15 to 25 GeV, a second one between 20 and 50 GeV. For the FEL, energies up to 30 GeV are being considered at this moment. After the beam is collimated both in energy and size, a fast kicker at the end of both beamlines will make it possible to distribute the electron beam to two undulator beam lines each, i.e. four lines in total (see Fig. 1). For each energy, one undulator has a fixed gap, the second has a variable gap. The wavelength to be generated in the fixed gap device determines the electron beam energy, whereas the gap in the second undulator determines, at this same energy, the wavelength for a second user. Therefore, both users can have an independently tunable wavelength at their disposal. While the electron beam produces the SASE FEL radiation, its energy reduces due to emission of synchrotron radiation. At the same time, the energy spread increases. Therefore, the beam can no longer be used to generate SASE radiation at the same wavelength. At longer wavelengths, however, it is still possible to

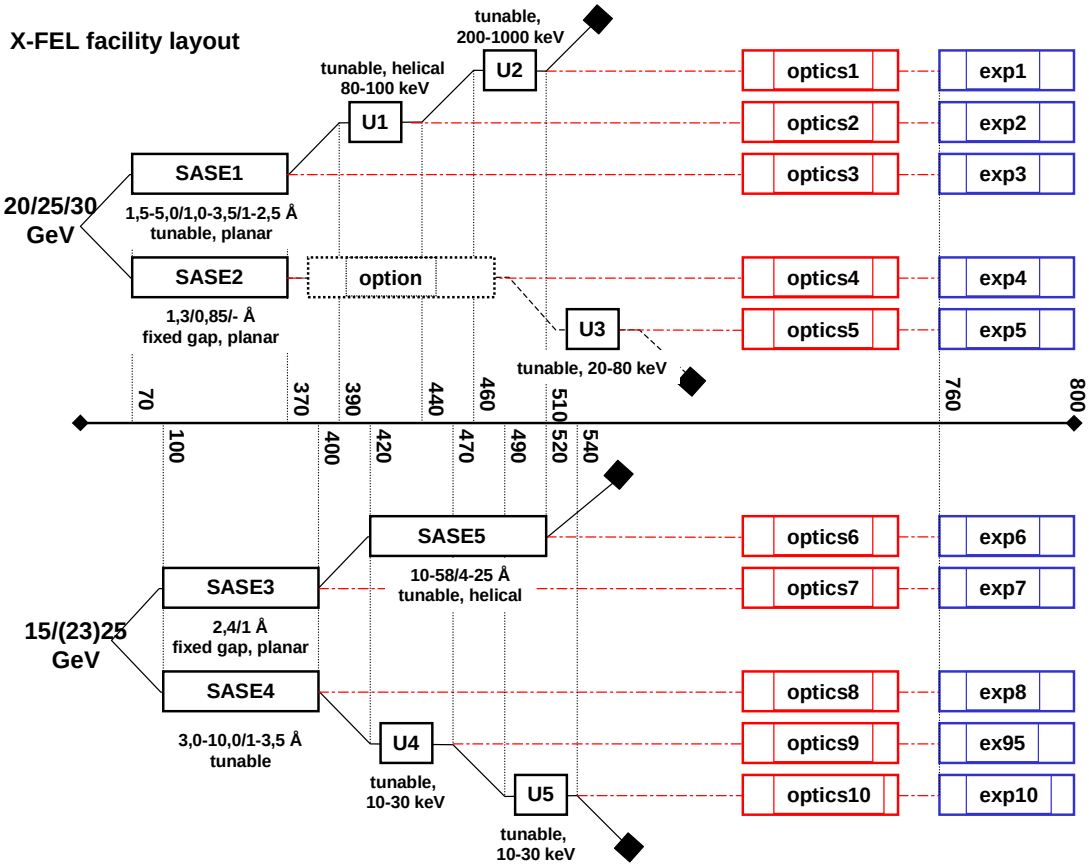


Fig. 1. Schematic layout of the TESLA X-ray FEL facility. The facility consists of four planar undulators in the short wavelength range (0.85 to 10Å) , one helical undulator at longer wavelengths (4 to 58 Å) and five spontaneous radiators. The future optional extension for a two-stage FEL to reduce the bandwidth is already shown.

produce intense SASE light. In addition, broadband spontaneous radiation, which does not suffer from reduced beam quality, can also be produced. Therefore, behind one undulator beamline (SASE-3), a second undulator is placed to produce SASE radiation at a longer wavelength (SASE-5), behind three (SASE-1, SASE-2 and SASE-4), spontaneous radiators are placed. Behind SASE-2, there is space for a so-called two-stage FEL option. This principle allows to narrow the FEL radiation bandwidth without reducing the output power, thus increasing the spectral brilliance by close to three orders of magnitude [2].

Because saturation has to be reached in a single pass, the electron beam has to be of high quality. This means that both transverse emittance and energy spread have to be small. Especially the normalized emittance of 1.6 $\pi$ mm mrad is a challenge, since this value is at the limit of what has been achieved so far. Furthermore, because the peak currents needed for the FEL cannot be achieved for any existing electron source, the beam has to be longitudinally compressed and transversely focused. For the beam parameters given in Table 1, the saturation length, and thus the minimum undulator length, has been calculated both analytically and with the use of simulation codes [3–5]. These simulations assume, however, that the electron beam is perfectly matched to the undulator optics and the undulator is ideal. In practice, components can be misaligned, the magnetic field is not perfect and the beam has some random variation of initial conditions, such as position, angle and energy. All these effects will reduce the gain and therefore increase the required undulator length.

A study on the influence of different kind of undulator imperfections has shown that the main effect is a reduc-

Table 1
Parameters used for the simulations presented in this report. The undulator parameters correspond to the SASE-1 undulator for an energy of 25 GeV.

| **Electron beam parameters** | |
|---|---|
| Electron beam energy, $\mathcal{E}$ | 25 GeV |
| Peak current, $I$ | 5.0 kA |
| rms bunch length | $25\ \mu$m |
| rms transverse beam size at 25 GeV | $38\,\mu$m |
| rms normalized slice emittance, $\epsilon_{\rm n}$ | 1.6 mm mrad |
| rms slice energy spread, $\sigma_{\rm E}$ | 2.5 MeV |
| **Undulator parameters for SASE-1** | |
| Period | 60 mm |
| Gap | 22 mm |
| $K_{\rm rms}$-parameter | 2.62 |
| Peak magnetic field | 0.67 T |
| Unit length | 5 m |
| Number of units | 53 |
| **FODO parameters** | |
| FODO period | 12.2 m |
| Quadrupole length | 200 mm |
| Quadrupole gradient | 20 T/m |
| Quadrupole focal distance | 20 m |

tion in overlap between electron beam radiation field [6]. As long as the electron beam has and rms deviation along the undulator of less than $7\,\mu$m, the reduction in the amplification is moderate. This alignment can be achieved if all quadrupoles have an offset smaller than $1\ \mu$m, as seen in Fig. 2.

In this report, a beam based alignment procedure that achieves this tolerance level is discussed. In addition, it is shown that the same procedure can be used to correct residual errors of the undulator end fields. In the following section, the alignment precedure is described. Section 3 shows simulated results of the alignment procedure to correct quadrupole offsets. Finally, the results are discussed and requirements on equipment is given.

## 2. The alignment procedure

Each undulator system with a total length of several hundred meters, consists of cells. Each cell is built up of an undulator segment, a phase shifter to match the phase of electrons and radiation field between segments [9], and a quadrupole of a FODO structure to keep the beam at a constant small diameter (see Fig. 3). The quadrupoles are placed on precision movers, but they are not remotely controlled in the present design. Alignment of the electron beam is performed using the last horizontal steerer of the phase shifter and the vertical steerer behind the quadrupole.

The initial alignment of the quadrupoles will be performed with an optical alignment system. So far, experience with this method shows that quadrupoles will be within $\pm 200\,\mu$m of a straight line. Due to the kicks by all quadrupoles, the electron beam orbit deviates from this line. The rms value of this deviation has been calculted for 1000 different random quadrupole distributions within the limits of $\pm 200\ \mu$m. The probability for a given rms orbit deviation is shown in Fig. 4. The distribution is very well fitted by a Rayleigh function. [1] It reaches its maximum value at $\sigma_b = 382\ \mu$m, with a tail up to 1.5 mm. The alignment of the electron beam therefore has to be improved by almost two orders of magnitude.

[1] The Rayleigh function is proportional to $x/\sigma^2 \cdot e^{-x^2/2\sigma^2}$ It has its maximum at $x = \sigma$.

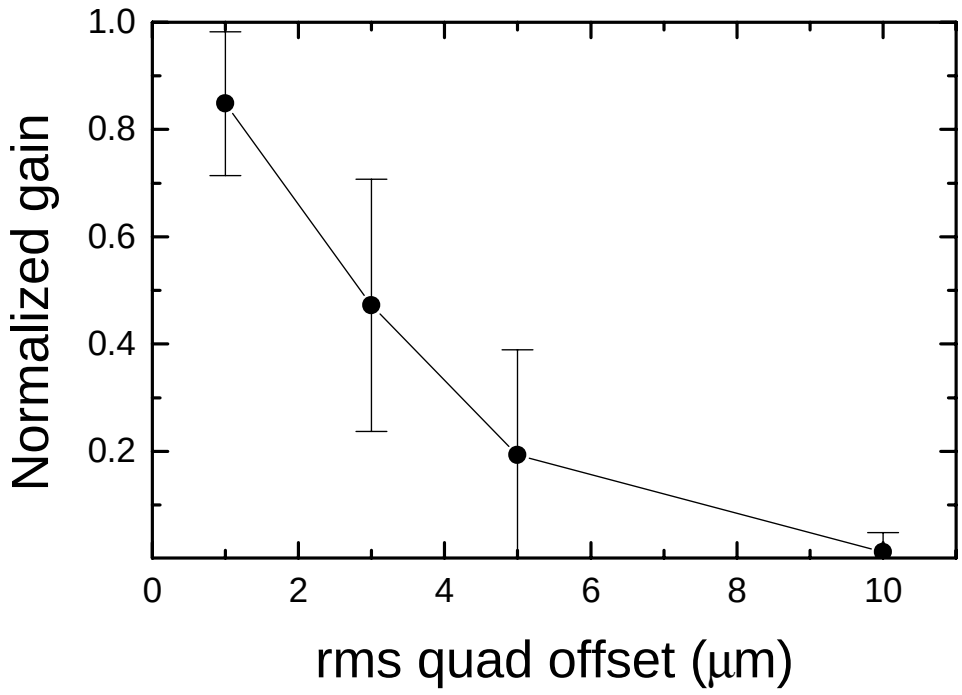


Fig. 2. Gain as a function of random quadrupole offsets. Simulations have been performed with parameters as given in Table 1, with the undulator tuned to a radiation wavelength of 1Å. Each point represents the averaged gain of 50 simulations normalized to the gain for an ideal undulator system. The quadrupoles are randomly positioned around the optical axis with a maximum offset as indicated. The error bars indicate the scatter of these simulations.

With as starting point the quadrupole offsets after pre-alignment, a number of steps have to be performed to obtained the required straightness of the electron beam trajectory.

(1) transport the electron beam to the beam dump.

(2) set the beam close the undulator axis at the entrance and the exit.

(3) determine the quadrupole offsets.

(4) correct the quadrupole offsets.

(5) correct first and second field integrals of the undulator segments.

As a first step in the alignment procedure, one has to get beam through the undulator beam pipe to the beam dump. In order to achieve this, the undulator gaps are opened to their maximum value. Thus, the on-axis magnetic field is negligible and therefore possible kicks due to non-zero field integrals are avoided. In order to avoid quadrupole kicks, all quadrupole gradients are also set to zero. Within this pure driftspace, the electron diameter will grow along the undulator. The growth of the $\beta$-function along the undulator is given by

$$\beta(z) = \beta_0 \left(1 + \frac{z^2}{\beta_0^2}\right), \tag{1}$$

where it is assumed that the waist is put at the undulator entrance. At the waist, $\beta_0$ is approximately 45 m. From the entrance to the end of the 300 m beam line the beam radius $\sqrt{\beta\epsilon}$ grows in both planes from $35\ \mu$m to $250\ \mu$m, which is still acceptable. It is now easy to correct the angle of the beam such that the beam dump is reached.

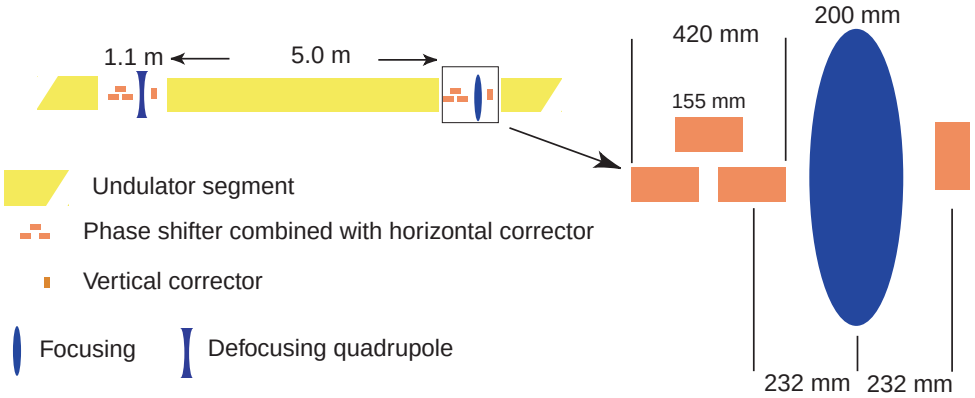


Fig. 3. Undulator cell of which the undulator system is built up. Shown are the phase shifter, the quadrupoles, the vertical steerer and an undulator segment. Not shown are the beam position monitors that will be positioned between the segments. An undulator system typically consists of an array of 53 of such cells.

As a second step, the electron beam has to be aligned to the optical axis of the undulator. A study on tolerance levels for the TESLA X-ray FEL has shown that the electron beam has to be along the magnetic axis of the undulator within the same 200 $\mu$m with which the quadrupoles are aligned [6]. Therefore, centering the electron beam in the first and last quadrupole is sufficient. This can simply be done by minimizing the kicks in both of them. A kick in the first quadrupole is caused by an initial offset of the beam, a kick in the last one by an initial angle. To correct the initial beam offset, the quadrupole gradient is changed from its zero value to its nominal value. If the electron beam is centered, none of the BPMs downstream from te quadrupole should show a change in position of the beam with changing gradient. Thus, the beam position is altered until a variation of the quadrupole gradient does not result in a different position reading in any of the BPMs. In a similar way, the angle is changed, keeping the initial beam position fixed, until a varying gradient in the last quadrupole does not change the readings in the BPMs downstream from it.

The beam now defines the required straight line. The next step is to determine the quadrupole offsets with respect to this line. They are determined one at a time, starting with the second quadrupole (the first one is already aligned: it defines the start of the straight line). All quadrupole gradient are still set to zero. The second quadrupole is now put to a value about 20% lower than nominal [2] .

The change in direction caused by the quadrupole kick is given by

$$x'_Q = \frac{\delta x}{f}\,, \tag{2}$$

with $f$ the quadrupole focal length and $\delta x$ its offset. The change in beam position $\Delta x_{\,BPM}$ measured by a BPM downstream from the quadrupole is

$$\Delta x_{BPM} = \frac{\delta x}{f} L\,, \tag{3}$$

with $L$ the distance between the BPM and the quadrupole. Eqs. (2) and (3) show that the kick depends on the focal length of the quadrupole. Therefore, changing the its focal length will be visible on the BPM by a change in position, unless the beam goes through the quadrupole on-axis. The beam at the quadrupole position is shifted using an upstream steerer (not the one directly in front in order to prevent too large angles). The beam position measured by the BPM shows a linear dependence on the applied current. After the steerer strength has been varied over a certain range, the quadrupole focal length is changed to a value of about 20% larger than nominal. Varying

[2] Since the center of a quadrupole varies with its strength, the variation has to be done around its nominal value [7].

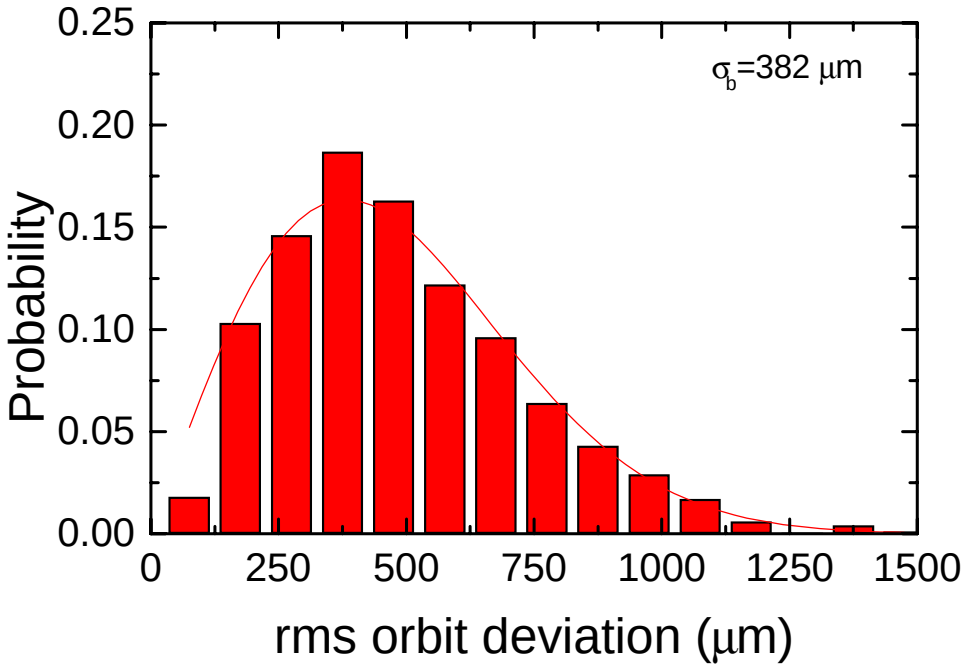


Fig. 4. Probability distribution of the rms orbit deviation for an electron beam that enters the SASE-1 FODO structure with zero initial angle and position for 1000 samples of randomly positioned quadrupoles. The quadrupoles have a random transverse offset within $\pm 200\ \mu$m. All other parameters are given in Table 1. The simulated rms orbit distribution is fitted with a Rayleigh function with $\sigma = 382\ \mu$m.

the steerer strength again gives another straight line. Because the quadrupole does not change the beam position that goes through its center, the two lines intersect when the steerer corrects the beam through the center, as is illustrated in Fig. 5. The quadrupole offset can now be calculated from the angle produced by the steerer. If the steerer is a distance $D$ upstream from the quadrupole and the BPM a distance $L$ downstream, the quadrupole offset is given by

$$\delta x = \frac{D}{D+L} \cdot \Delta x_{BPM} \approx x'_s \cdot D\,. \tag{4}$$

This procedure has to be performed for each quadrupole, every time setting the others to zero gradient.

With all the quadrupole offset known, the beam can in principle be corrected. The kick produced by the quadrupole can be corrected by the steerer. For this correction, the steerer close to the quadrupole is used. With $d$ the distance between steerer and quadrupole, the angle by the steerer is $x'_s = \Delta x_{beam}/d$, with $\Delta x_{beam}$ the beam shift at the quadrupole position. This angle has to be equal to the kick produced by the quadrupole, but of opposite sign, i.e. $x'_s = -x'_Q$. With the kick of the quadrupole given by $x'_Q = (\delta x - \Delta x_{beam})/f$, one finds that the beam offset needed is

$$\Delta x_{beam} = \frac{d}{d-f} \cdot \delta x \approx -\frac{d}{f} \cdot \delta x\,, \tag{5}$$

since $d \ll f$. For typical values $d = 232\,$mm (see Fig. 3) and $f = 20\,$m (see Table 1), this is about 1% of the quadrupole offset. For a random quadrupole offset within $\pm 200\ \mu$m, the beam offset varies within $\pm 2\ \mu$m. This is already a significant fraction of the tolerable orbit deviation of $7\ \mu$m. Since aligning the beam through the quadrupoles and undulator field errors will add to the deviation, this offset should be corrected by shifting the quadrupoles. After the quadrupoles have been shifted to offsets that are an order of magnitude smaller, the beam offset will no longer contribute significantly to the total beam deviation. The entire last step has to be repeated in order to check residual quadrupole offsets. After the new offsets are known, they can be corrected using the steerers

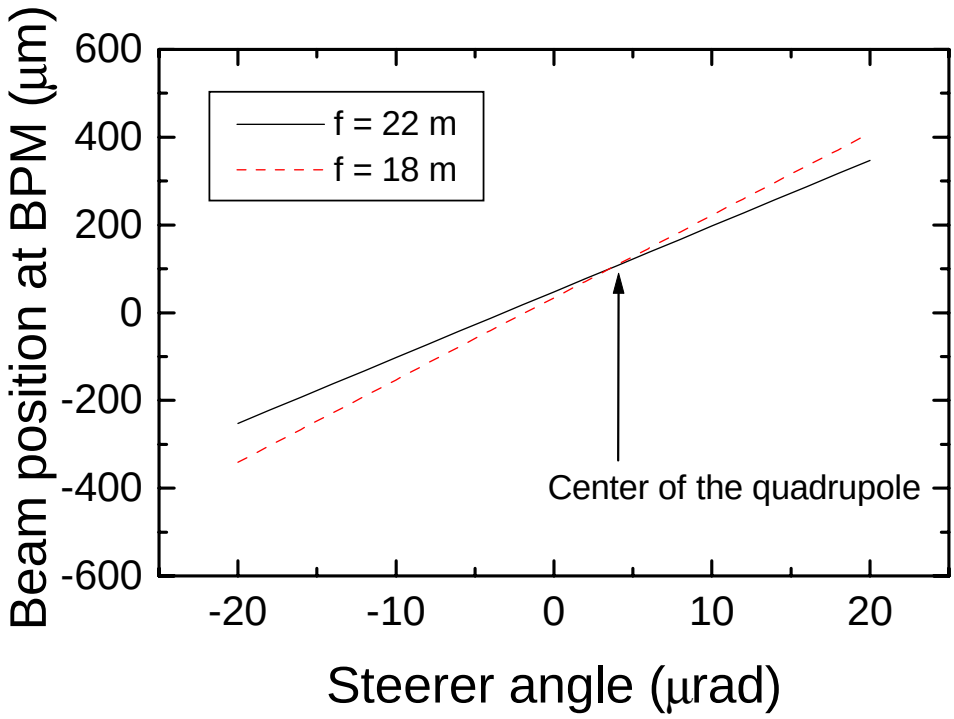


Fig. 5. Beam position measured by a BPM downstream of a quadrupole as function of the angle produced by a steerer in front of the quadrupole. Each line corresponds to a variation in applied current in an upstream steerer. The two different lines are for different focal lengths of the quadrupole. The two lines intersect when the beam is going through the center of the quadrupole, in which case the quadrupole does not kick the beam.

as described before. Note that during the entire procedure, the BPMs do not have to be calibrated. The quadrupole offsets are determined by geometrical factors, such as distance between corrector and quadrupole and between quadrupole and BPM, and the angle made by a corrector with a given strength. The lengths can be measured accurately, the corrector can be calibrated (field for applied current) and the energy can be determined. Errors in these quantities lead to an error in the calculated quadrupole offset. However, the correctors are used to do the final correction.

With this procedure performed twice, once to determine by how much the quadrupoles have to be shifted and the second time to correct quadrupole residual kicks still present, the first and second field integrals of the undulator segments have to be corrected. The field integrals will be measured as a function of gap onb a magnetic bench before the segments are put in their final place. Therefore, one can assume that only small unknown effects have to be corrected. Most likely, only some small final kick, i.e. non-zero first field integral has to be compensated. This can easily be done by closing the undulator gaps in sequence, starting upstream. With all quadrupoles set to zero, an angle of the electron beam leaving the undulator can be seen downstream and corrected. In the unlikely case that a second field integral has to be corrected, one can use the quadrupole just behind the segment. A small offset results again in an angle which becomes visible downstream. Before continuing with the next undulator segment, photon beam based alignment will be used to determine accurately the undulator gap and the value needed for the phase shifter by looking at the spontaneous emission produced by the electron beam.

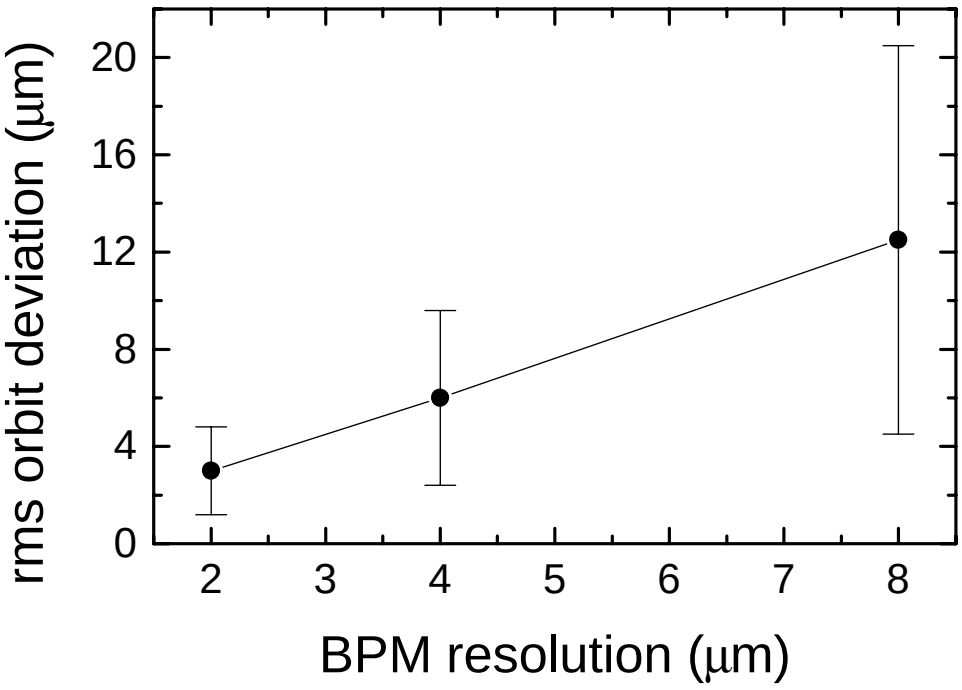


Fig. 6. Rms value of the orbit deviation after beam based alignment of the quadrupoles. Errors due to undulator errors and offset of the electron beam due to different position of corrector and quadrupole are not included. Each point corresponds to 1000 simulations with different initial quadrupole distributions. The parameters parameters used are given in Table 1.

### 3. Result of the Beam Based Alignment of Quadrupoles

The first two steps in the previous section will not be repeated here. Alignment of the beam, either by shifting the quadrupoles or by using the steerers, require the same measuring method. Therefore, the procedure is performed once, assuming that the quadrupole offsets are small enough and the beam offset needed for corrections are negligibly small. The simulations have used the BPM 18.3 m downstream from the quadrupole that has to be corrected. The angle produced by the steerer gives a maximum beam offset of $\pm 100$ $\mu$m at the quadrupole position.

The beam based alignment procedure has been simulated for 1000 different samples of random distributions of quadrupole offsets. Results are shown in Fig. 6 as a function of BPM resolution. For a resolution of 2 $\mu$m, the orbit deviation is $\sigma_b = 3$ $\mu$m. This is an improvement by more than a factor 100 compared to the rms deviation of the orbit before alignment. For this resolution, the rms value of the distribution of orbit deviation for 1000 samples is shown in Fig. 7. It has again been fitted with a Rayleigh function. The probability that the orbit deviation is larger than a given value $s = 7$ $\mu$m is given by $e^{-s^2/2\sigma^2}$. The figure shows that almost 95% of corrected orbits are within this limit. If the quadrupoles are physically shifted to offsets smaller than $\pm 20$ $\mu$m, this value is not visibly changed by the offset of the beam from segment to segment. With the undulator field integrals corrected for each segment, the kicks within each segment due to magnetic (peak) field errors will only give a minor contribution to the orbit deviation.

As discussed in the previous section, all quadrupole gradients are set to zero except for the one of which the offset is determined. Similar simulations performed with all gradients to their nominal value resulted in a 5 times larger orbit deviation for the same BPM resolution. This is due to residual kicks caused by previously aligned upstream quadrupoles. The orbit deviation from a straight line grows along the undulator. This is visible as a steady increase in the corrector strength needed to compensate for quadrupole kicks. Although this can be corrected, one

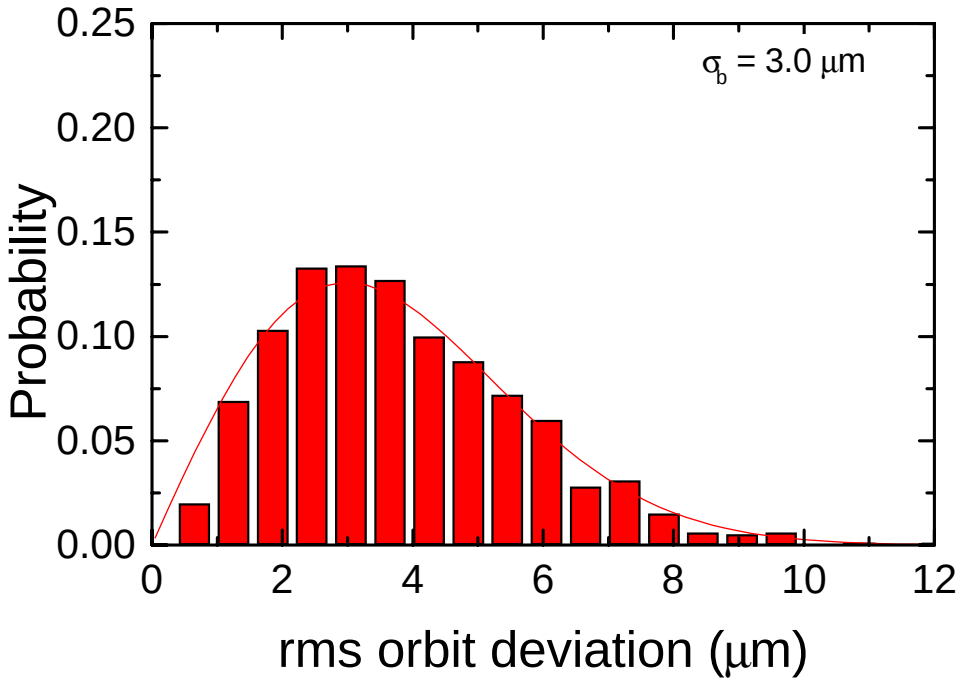


Fig. 7. Probability distribution of the rms orbit deviation for 1000 samples of quadrupole offsets. The electron beam enters the SASE-1 FODO structure with zero initial angle and position. The quadrupoles initially have a random transverse offset with an rms value of $\pm 200$ $\mu$m. The difference in offset from undulator segment to segment due to different position of corrector and quadrupole is not included. The BPM resolution is 2 $\mu$m. All other parameters are given in Table 1.

does not reach the level that is possible with the method proposed here [8].

Results of the alignment procedure have been shown for the SASE-1 undulator at a given electron beam energy of 25 GeV. However, the focal length is chosen independent of energy. Therefore, so are the kicks produced by quadrupoles. At lower energy, the electron beam size will be larger, which increases the acceptable tolerance level. Hence, the highest energy gives the tightest requirements. This is also true for the other undulators. For the SASE-5 undulator, the $\beta$-function is smaller. The tolerances are therefore more tight, namely of the order of $4.5$ $\mu$m. Even in this case, 80% of all orbits is within tolerances.

## 4. Discussion and Conclusions

It has been shown that the quadrupoles can be aligned within the required accuracy using beam based alignment. In order to achieve this, all quadrupoles have to be set to zero with the exception of the one that is being aligned. The BPM resolution needed is approximately 2 $\mu$m. After the quadrupoles are aligned, the BPM positions with respect to the straight line are known. Therefore, kicks of the undulator field due to non-zero first and second field integrals can be corrected. This is done by closing the gaps one by one. With all quadrupoles set to zero, a non-zero first field integral produces an angle. A non-zero second field integral produces a kick in a downstream quadrupole, which can be measured at the end of the beamline.

A number of machine parameters, such as lengths, distances and calibration of steerers have to be known. Errors in those values will lead to errors in the final alignment. In order to determine the amount by which the quadrupoles have to be shifted, one has to know the distance between steerer and quadrupole, and between quadrupole and

BPM. Errors in those distances will lead to a wrong shift of the quadrupole. Since it is a linear dependence, the error made will only be a minor one.

In order to correct with the steerer the small offset after the quadrupole has been shifted, its field has to be known. The corrector field needed is $B\ell_s = Q\ell_Q\delta x$, with $Q$ the quadrupole gradient, $\ell_s$ and $\ell_Q$ the steerer and Quadrupole length, respectively. From beam based alignment, $\delta x$ is known as the position where the quadrupole is steering free. It can be estimated within a $\mu$m level. The error made in the corrector strength will be mainly due to an error made in determining the quadrupole gradient.

An other pint is the stability of the beam after alignment. First of all, beam jitter has to be small compared to the $7\,\mu$m tolerance level. With a dynamic range of the steerers of $\pm 400\,\mu$m, they need a stability of the order of 0.1% in order to remain in the sub-micrometer range. This is well within what is achievable.

With the electron beam aligned, the BPMs can be calibrated. This should reduce the frequency with which the beam based alignment procedure has to be performed. Because of the tight tolerances, it is still needed on a regular basis. When it is done with steerers, no parts have to be moved mechanically and the procedure is rather fast. The procedure has to be performed in such a way, however, the hysteresis does give an offset to the beam because of different fields at he same current. This could for example mean that the corrector always has to be changed from the same direction. Only if the quadrupole offsets exceed the $20\,\mu$m limit, they have to be moved again. At this moment it is not clear how often this has to be done (dependence on movement of foundation, etc.) In case this procedure is needed too often, the system does allow to add a remotely controlled system.

A number of points have not been addressed. For example, if the alignment of the beam through the quadrupoles has an angle which is too large with respect to the undulator optical axis. This would be visible, however, when all the quadrupoles are switched off. If the effect is significant, the angle would show up as a betatron oscillation.

Additional effects, such the influence of beam jitter and dispersion at the undulator entrance are still under study. Also the influence of the finite lens thickness is under study. However, studies for the TTF-FEL have shown that most of these problems can be solved [8,10].

**Acknowledgement:**

The author would like to thank P. Castro, J. Pflüger, P. Piot, E.L. Saldin, E.A. Schneidmiller, M. Tischer and M.V. Yurkov for their useful comments.

## References

[1] *"A VUV Free Electron Laser at the TESLA Test Facility: Conceptual Design Report"*, DESY Print TESLA-FEL 95-03, Hamburg, DESY (1995)

[2] J. Feldhaus et al., Opt. Commun. **140**, (1997) 341.

[3] E.L. Saldin, E.A. Schneidmiller, M.V. Yurkov, *The Physics of Free Electron Lasers*, Springer, Berlin-Heidelberg (2000) and references therein.

[4] E. L. Saldin, E. A. Schneidmiller, and M. V. Yurkov, Nucl. Instrum. and Methods A**429**, (1999) 233.

[5] S. Reiche, Nucl. Instrum. and Methods A**429**, (1999) 243.

[6] B. Faatz, J. Pflüger, *"Field Accuracy Requirements for the Undulator Systems of the X-ray FEL's at TESLA"*, DESY Print TESLA-FEL 2000-14, Hamburg, DESY (2000)

[7] P. Tenenbaum and T.O. Raubenheimer, Resolution and Systematic limitations in beam-based alignment, Phys. Rev. Special topics (2000)

[8] K. Flöttmann, B. Faatz, E. Czuchry and J. Roßbach, Nucl. Instrum. and Methods A**416**, (1998) 152.

[9] J. Pflüger, M. Tischer, *"A Prototype Phase Shifter for the Undulator Systems at the TESLA X-ray FELs"*, TESLA-FEL 2000-08, DESY (2000)

[10] P. Castro *"TTF FEL Beam Based Alignment by dispersion correction using Micado Algorithm"*, DESY Print TESLA-FEL 97-04, Hamburg, DESY (1997)